

Nils Lundgren · Mats Ekevad · Jens Flodin

Choosing green sawing dimensions for Norway spruce from stochastic simulations

Received: February 15, 2010 / Accepted: June 23, 2010 / Published online: October 7, 2010

Abstract The high accuracy of log positioning and the stability of saw blades in breakdown machinery in modern sawmills have reduced the need to add margins for sawing variations. Oversize green sawing dimensions are still needed, but mainly to allow for drying shrinkage. This has put a new focus on better adapting green sawing dimensions to the shrinkage behavior of wood. In this study, a method for optimization of green sawing dimensions using stochastic simulation is presented. Normal distributions were generated for planed dry dimensions, kerf width, and target moisture content. The minimum share of boards exceeding the specified dry dimensions was decided, and deformations in boards from all positions in the cross section in a number of logs were simulated. The simulated shrinkage allowance from stochastic simulations was compared to experimental results from an industry test and to finite element results based on material data for Norway spruce. The results showed that the green width of the sawn boards should increase when the number of boards in the center yield increases. The green thickness of boards should be thinner for center boards and outer boards than for inner boards.

Key words Norway spruce · Drying · Stochastic simulation · Shrinkage · Wood

Introduction

The margins that are added to nominal lumber dimensions should compensate for sawing variations and for dimensional changes and deformations in the sawn lumber arising from shrinkage during drying. The main deformation of

the cross section is cupping caused by differences in the radial and tangential shrinkage in wood. In spruce, the amount of tangential shrinkage is approximately twice that of the radial shrinkage.¹ This means that the thickness and width shrinkage and the amount of cupping will depend on the position within the cross section of the log, as shown in Fig. 1.

The increasing accuracy in log positioning and consistency in kerf width in modern sawmills reduces the need to compensate for sawing variations, but margins are still needed to allow for shrinkage during drying.² Today, sawmills often use the same margins for all boards, but if individual margins are used for each board, it will be possible to increase yield by producing the same dimensions from logs with smaller diameters. When the radial and tangential shrinkage coefficients are known, it is possible to analytically calculate the dry dimensions for boards from different positions in the cross section of the log.³ Normally, the dry dimensions are specified and the green sawing dimensions have to be calculated. This article presents a method for finding the green sawing dimensions by the use of stochastic simulation. The algorithm is related to experimental data and was verified using the finite element method (FEM). Only plane cross-section deformation was considered, and not drying deformations along the length of the boards such as crook, bow, and twist.

Materials and methods

Experimental material

The study was based on data obtained by industrial measurements of green and dry dimensions for boards sawn from Norway spruce logs [*Picea abies* (L.) Karst.] at a Swedish sawmill. The sawing patterns used gave a center yield of 2, 3, or 4 boards (denoted 2EX, 3EX and 4EX, respectively). The saw logs were selected from three log size classes with 21 logs in each class, and the sawing pattern was decided by the log size according to Table 1. This gave a total of 189 boards with dry dimensions 51 × 149 mm.

N. Lundgren (✉) · M. Ekevad
Luleå University of Technology, Division of Wood Science and Technology, LTU Skellefteå, SE-931 87 Skellefteå, Sweden
Tel. +46-910-585756; Fax +46-910-585399
e-mail: nils.lundgren@ltu.se

J. Flodin
SP Technical Research Institute of Sweden, Wood Technology, Skeria 2, SE-931 77 Skellefteå, Sweden

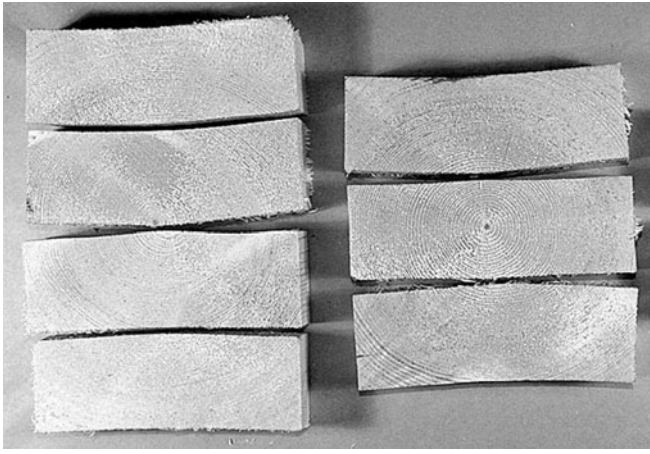


Fig. 1. Deformations after drying to 7% moisture content in cross sections of boards sawn from Norway spruce with 4EX (left) and 3EX (right) square sawing pattern

Table 1. Log size classes and sawing patterns used in this study

No. of logs	Top diameter (mm)	Sawing pattern (center yield)
21	190–200	2EX log 51 × 149 mm
21	225–235	3EX log 51 × 149 mm
21	270–280	4EX log 51 × 149 mm

The sawn boards were dried in a batch kiln and the average moisture content (MC) after drying was measured as 7.3% with a standard deviation of 0.44%. Green and dry dimensions for each board were measured with a digital caliper at 300 mm from the top end of the boards. The measurements were made between the stickers that separate the layers of boards, and this means that cross-sectional deformation was comparable to deformation in free drying.

An earlier study⁴ based on the same experimental data concluded that the main influence on shrinkage was the pith position in the cross section and that the density (i.e., the growth rate) had a very small effect on shrinkage. The general agreement between the analytically calculated shrinkage, the FEM simulation results with different material models, and experimental results has been previously reported.⁵

Analytic calculations

Using the radial and tangential shrinkage coefficients, it is possible to calculate the stress-free deformation of a cross section if the pith is located outside the cross section.³ The width shrinkage on the sapwood side (w_s), width shrinkage on the pith side (w_p), shrinkage in edge thickness (t_e), and shrinkage at mid-thickness (t_m) were calculated as:

$$w_s = b \cdot \left(1 - k_r \sqrt{1 + \frac{4a^2}{b^2} \sin^2 \left(\frac{k_t}{k_r} \tan^{-1} \left(\frac{b}{2a} \right) \right)} \right) \quad (1)$$

$$w_p = b \cdot \left(1 - k_r \sqrt{1 + \frac{4(a-c)^2}{b^2} \sin^2 \left(\frac{k_t}{k_r} \tan^{-1} \left(\frac{b}{2(a-c)} \right) \right)} \right) \quad (2)$$

Table 2. Random distributions for the simulation

Distribution	Average value	Standard deviation
Cant saw, kerf width (mm)	4	0.3
Ripsaw, kerf width (mm)	4	0.3
Radial shrinkage coefficient k_r	0.9619	0.0083
Tangential shrinkage coefficient k_t	0.9274	0.0107
Target moisture content	Experimental values for each sawing pattern	

$$t_e = c \cdot \left(1 - k_r \frac{a}{c} \left[\sqrt{1 + \frac{b^2}{4a^2} \cos^2 \left(\frac{k_t}{k_r} \tan^{-1} \left(\frac{b}{2a} \right) \right)} - \sqrt{\left(1 - \frac{c}{a} \right)^2 + \frac{b^2}{4a^2} \cos^2 \left(\frac{k_t}{k_r} \tan^{-1} \left(\frac{b}{2(a-c)} \right) \right)} \right] \right) \quad (3)$$

$$t_m = c \cdot (1 - k_r) \quad (4)$$

where k_r is the radial shrinkage coefficient (oven-dry length/green length), k_t is the tangential shrinkage coefficient (oven-dry length/green length), a is the distance from the pith to the sapwood side of the board, b is the green board width, and c is the green board thickness.

Cupping was calculated as:

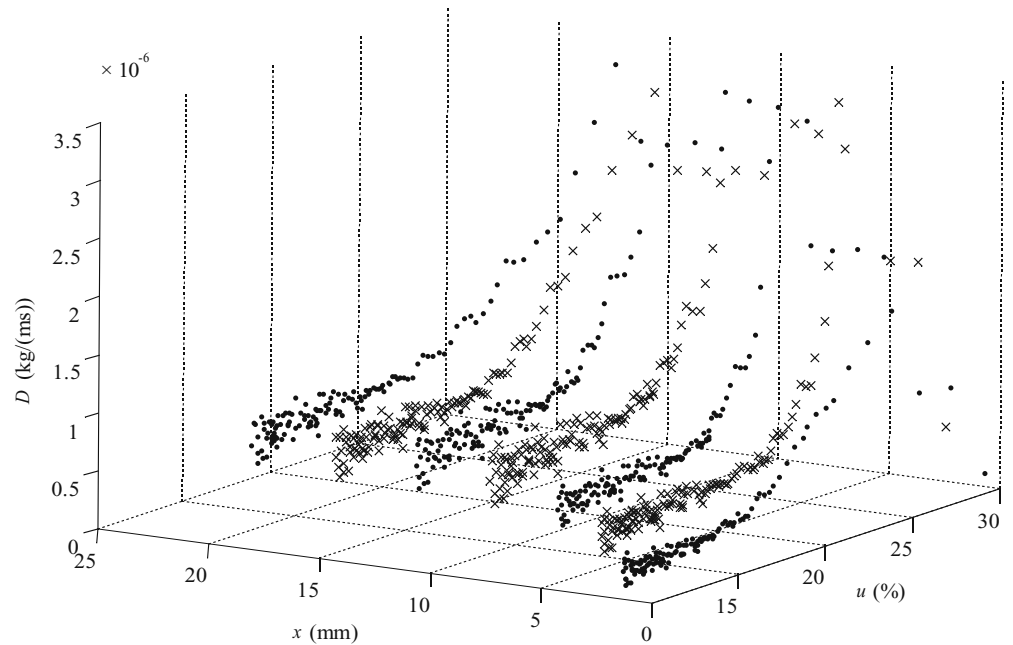
$$cup = k_r a \cdot \left(\sqrt{1 + \frac{b^2}{4a^2} \cos^2 \left(\frac{k_t}{k_r} \tan^{-1} \left(\frac{b}{2a} \right) \right)} - 1 \right) \quad (5)$$

The calculated values were comparable to results from an elastic FEM model, except for the 3EX center board, for which the pith was in the middle of the cross section. The analytical expressions are not applicable to 3EX center boards due to the stress induced. Also, the analytical method is only valid if the MC in the cross section is assumed to be constant. However, in the current study, 3EX center-board analytical values were calculated by splitting the board in two (i.e., with half the thickness). A fictitious 3EX center board was constructed by mounting the two halves together after drying. Cupping for the 3EX center board was measured as half of the difference between the mid-thickness and edge thickness.

Stochastic simulation

The minimum values for green sawing dimensions were calculated by stochastic simulation.⁶ Random normal distributions with average values and standard deviations were generated from experimental data (Table 2) for target moisture content, radial and tangential shrinkage coefficients, and kerf width for the saw blades. Initial estimations of green dimensions were made from the specified dry dimensions. Sawing was then simulated for a number of boards, and the deformation during drying was calculated from the analytic expressions given in Eqs. 1–5. The green dimensions were adjusted and the simulation was repeated until the specified dry dimensions were reached for a specified share of the boards.

Fig. 2. The diffusion coefficient D as a function of distance from the surface x and moisture content u . u is the driving potential. From Danvind and Ekevad⁷



The algorithm is summarized in the following four steps:

1. Generate random distributions ($n = 400$) according to Table 2.
2. Set green dimensions for the cant equal to the dry target dimensions for the boards plus the average width for each saw kerf.
3. Use the random distributions from step 1 together with the cant dimensions from step 2 to calculate dry board dimensions using Eqs. 1–5 for boards sawn from 400 cants.
4. Increase the green dimensions for the cant and repeat step 3 until the specified share of boards with dimensions exceeding the dry target dimensions is reached.

FEM simulations

Simulations using FEM give a detailed description of the moisture content u as a function of time and also indicate how the induced stress and dimensional changes of the boards vary during drying (u is water mass/oven-dry wood mass). The final dimensions after completing the drying schedule were used in this study for comparisons of the influence of different board positions in the cross section of the log.

In the first step, the drying process was simulated using an isothermal two-dimensional finite element (FE) diffusion model. The diffusion coefficient (Fig. 2) and the mass transfer coefficient were taken from earlier experiments⁷ valid for Norway spruce [*Picea abies* (L.) Karst.]. The drying schedule was aimed at 7% final MC after 120 h drying (Fig. 3). The commercial FE program ABAQUS⁸ was used together with user subroutines to model wood as an orthotropic material. The orthotropic axes were modeled in a cylindrical coordinate system and no spiral grain was

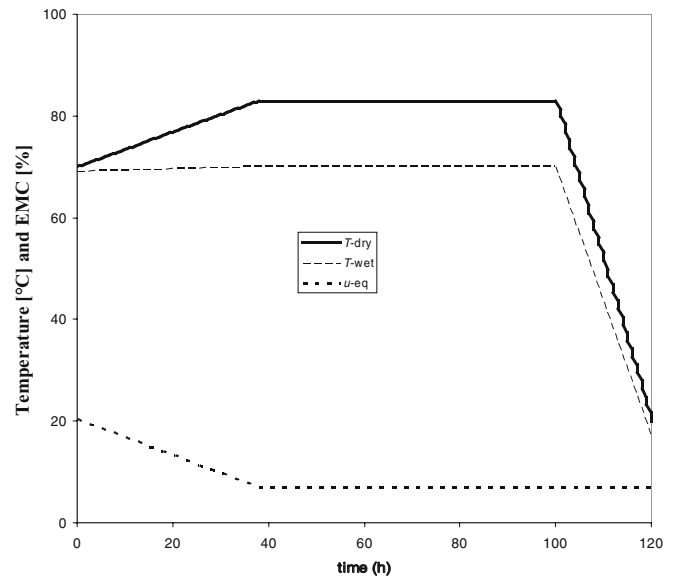


Fig. 3. Dry and wet temperature ($^{\circ}\text{C}$) and equilibrium moisture content (EMC) in percent for the drying schedule, which gives a final MC of about 7% after 120 h

assumed. The results from the first step were the distribution of MC in the body as a function of time.

Then, in the second step, the stresses, strains, and displacements (as functions of time) were calculated using the previously calculated distribution of MC as input. An elastic-mechanosorptive material model was used. The elastic orthotropic material model and the material coefficients for Norway spruce are shown in the appendix. Mechanosorption was induced via an added nonelastic mechanosorptive strain increment $m\sigma_{\text{dul}}$, where m was 0.15, 0.2, and 0.0001 (1/MPa) in the radial, tangential, and

Table 3. Measured average dimensions in green and dry conditions and final moisture content (MC)

Sawing pattern	Width sap side (mm)				Edge thickness (mm)				Cup (mm)		MC (%)	
	Green		Dry		Green		Dry		Dry		Dry	
	Value	SD	Value	SD	Value	SD	Value	SD	Value	SD	Value	SD
3EX in	156.6	0.2	151.8	1.1	53.6	0.2	50.2	0.3	0.58	0.47	7.56	0.37
2EX in	156.5	0.2	149.4	0.9	53.7	0.3	50.6	0.4	1.92	0.52	7.43	0.31
3EX out	156.7	0.3	147.8	0.9	53.6	0.3	51.0	0.4	1.74	0.51	7.50	0.40
4EX out	156.5	0.3	148.0	1.3	53.5	0.3	50.8	0.4	1.90	0.65	7.06	0.42
All Boards	156.6	0.3	148.7	1.6	53.6	0.3	50.7	0.4	1.72	0.72	7.30	0.44

longitudinal directions, respectively.⁹ A more detailed description of the FE model is given by Ekevad.¹⁰

Optimization of dimensions

Two different methods were used to find the optimal green dimensions. In the first method, the minimum width on the sapwood side and the planed thickness (edge thickness minus cupping) fulfilled by 99% of boards were chosen as the starting values, and green dimensions for each sawing pattern and position in the cross section were simulated using the analytical expressions and stochastic simulation.

In the second method, FEM was used to find the shrinkage for each sawing pattern and position. To find the best green sawing dimensions, the calculated shrinkage was added to the average measured dry dimensions for all boards.

Results

The measured average values for dimensions in the green and dry conditions and for MC in the dry condition are presented in Table 3. After drying, the average width for all boards was 148.71 mm, and the average planed thickness was 49.01 mm. These values were used as target dimensions for each position and sawing pattern in the FEM analysis. The width exceeded by 99% of all boards was 145.5 mm, while the planed thickness exceeded by 99% of all boards was 47.1 mm. These values were used as the target dimensions for 99% of the boards for each position and sawing pattern in the stochastic simulations.

The optimal sawn dimensions according to FEM and stochastic simulation for each sawing pattern are presented in Figs. 4 and 5, together with average measured values. The sawing patterns used at the sawmill were set with equal width and thickness for all boards, resulting in approximately the same measured values for all sawing patterns. The FEM and simulated values show that individual green target dimensions for each board in a sawing pattern can be used to increase the yield. The FEM and simulated results differ in the absolute values obtained, but the general trends are in agreement.

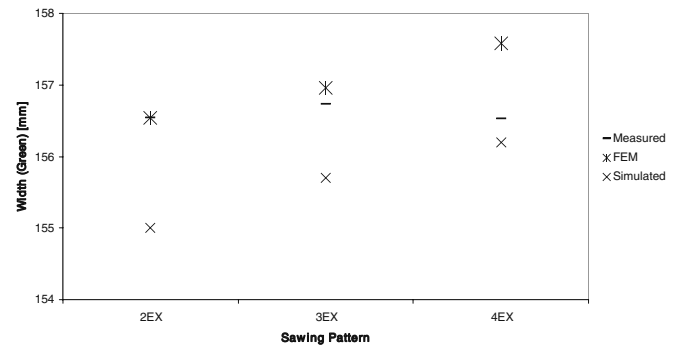


Fig. 4. Measured width in the green condition compared to the green width needed for each sawing pattern according to stochastic simulation and finite element method (FEM) simulation

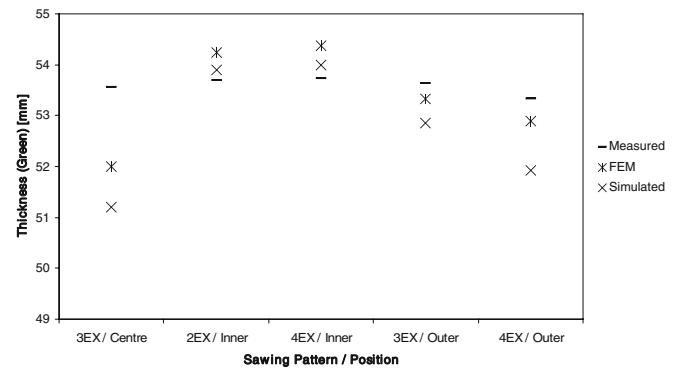


Fig. 5. Measured thickness in the green condition compared to the thickness needed for each sawing pattern according to stochastic and FEM simulations

Discussion

Using square sawing, the sawn width for center or inner boards from a log was the same as for the outer boards, while the thickness could be optimized in all positions. The differences between the results from FEM and stochastic simulations were mainly caused by the different values for the shrinkage coefficients. The coefficients used in the stochastic simulation were estimated from the experimental data, while FEM coefficients were based on literature values for Norway spruce. It is believed that FEM should give

Table A1. Elastic material coefficients at 20°C and 20% MC (estimated from the literature¹¹)

E_1 (MPa)	E_2 (MPa)	E_3 (MPa)	G_{12} (MPa)	G_{13} (MPa)	G_{23} (MPa)	ν_{12}	ν_{13}	ν_{23}
425	249	11390	34.2	729	695	0.418	0.00707	0.00521
β_{01}	β_{02}	β_{03}	α_{01}	α_{02}	α_{03}			
0.133	0.267	0.000	0.000	0.000	0.000			

E , elastic moduli; G , shear moduli; ν , Poisson's ratios; β , moisture expansion coefficients; α , temperature expansion coefficients

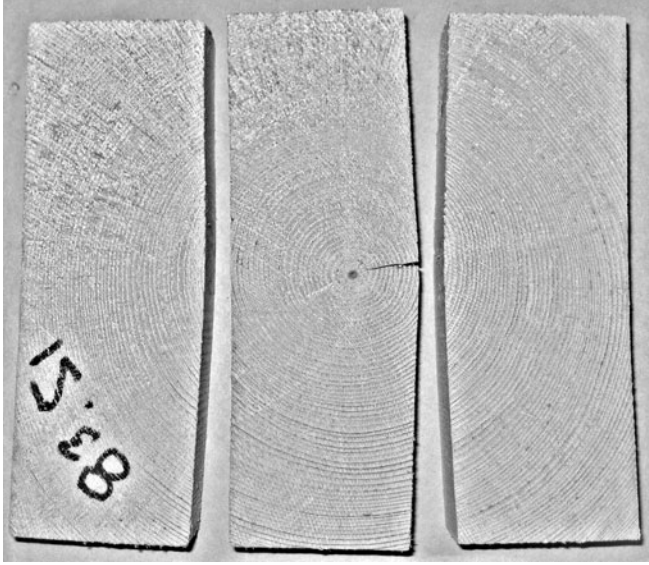


Fig. 6. Deformations after drying to 7% moisture content in cross sections of boards sawn from Norway spruce with a 3EX square sawing pattern

more accurate results (compared to the analytic calculations used in the stochastic simulations) when constraints are applied during drying because FEM takes the induced stresses into consideration. The pith was assumed to be centered in 3EX center boards. If the pith is closer to one side, there will be a cupping of the center boards (Fig. 6.) These boards are more likely to crack due to the induced stress.

Both methods show that center and outer boards should be sawn thinner than inner boards and that the sawn width should be increased with the number of boards in the center yield. The boards were dried to a low MC (about 7%) and the differences in recommended green thickness between positions in Fig. 5 are larger than they would be for a normal target MC. There will be less constraint on thinner boards when different thicknesses are mixed in the kiln, but the variations in thickness are believed to be too small to have significant influence on warp or twist.

Appendix: material coefficients used in the FE simulations

A summary of the three-dimensional orthotropic elastic material model and the numerical values of the material

parameters that were used are given here. The model was fully described by Ekevad.¹⁰ The material parameters are functions of temperature and MC.

Orthotropic directions for the material description are derived from a cylindrical coordinate system r - ϕ - z with the origin in the pith position and with the longitudinal z -direction along the pith (normal to the cross section of the board). Radial and tangential directions follow from this definition. The basic notation used below is that indices 1, 2, and 3 stand for radial, tangential, and fiber (longitudinal) directions, respectively. For stress and strain, a vector notation is used where the vectors are of size 6 and where the indices 1–6 indicate the normal directions 1, 2, and 3 and the shear directions 12, 13, and 23, respectively. An elastic modulus vector of size 6 is defined where the indices 1–6 indicate the elastic moduli in the normal directions E_1 , E_2 , and E_3 and the shear modulus G_{12} , G_{13} , and G_{23} , respectively.

The elastic relation between stress and strain follows from the definition of the elastic strain increment vector, which is modeled as:

$$d\bar{\epsilon} = \bar{F}d\bar{\sigma} + \bar{\alpha}_0dT + \bar{\beta}_0du - \bar{F}(\bar{M}_T\bar{\sigma}dT + \bar{M}_u\bar{\sigma}du),$$

where vectors (with overbars) are of size 6 and matrices (with two overbars) are of size 6×6 and where \bar{F} is the linear elastic flexibility matrix, $\bar{\alpha}_0$ is the temperature expansion coefficient, $\bar{\beta}_0$ is the moisture expansion coefficient, and \bar{M}_T and \bar{M}_u are the matrices containing relative gradients of elastic moduli, E , with respect to temperature and MC, respectively. Elastic material coefficients at $T = 20^\circ\text{C}$ and $u = 20\%$ are given in Table A1.

The variation of material coefficients with temperature and MC are specified as linear variations.

Poisson's ratios ν_{ij} were set as constants, and symmetry gives $\nu_{ij}/E_i = \nu_{ji}/E_j$ for $i, j = 1, 2, 3$. The moisture expansion coefficients β_1 , β_2 , and β_3 were constant, as the values specified in Table A1 for $u < 0.3$ and zero for $u > 0.3$. The temperature expansion coefficients α_1 , α_2 , and α_3 were constants, see Table A1.

The variations with T and u for all E and G components were accounted for by linear functions f_i and g_i , as $E_i(T, u) = E_i(T = 20^\circ\text{C}, u = 20\%) \cdot f_i(T) \cdot g_i(u)$ for $i = 1, 2, \dots, 6$. The gradients of the linear functions f_i were for $i = 3$ $\frac{\partial f_3}{\partial T} = -0.00233 \frac{1}{^\circ\text{C}}$ and for the other components ($i = 1, 2, 4, 5, 6$), $\frac{\partial f_i}{\partial T} = -0.011 \frac{1}{^\circ\text{C}}$. The gradients of the linear func-

tions g_i were for $u < (u_{\text{fsp}}-0.04)$ and $i = 3$ $\frac{\partial g_3}{\partial u} = -0.7344$ and for $u < (u_{\text{fsp}}-0.04)$ and $i = 1,2,4,5,6$ $\frac{\partial g_i}{\partial u} = -4.67$. The gradients of the linear functions g_i were zero for all components, i.e., $g_i = g_i(u = u_{\text{fsp}}-0.04)$ for $u > (u_{\text{fsp}}-0.04)$. The fiber saturation point was set as $u_{\text{fsp}} = 0.3298-0.001 \cdot T$ (T in $^{\circ}\text{C}$).

References

1. Dinwoodie JM (2000) Timber: its nature and behaviour, 2nd edn. E&FN Spon, London
2. Vuorilehto J (2001) Size control of sawn timber by optical means in breakdown saw machines. Doctoral Thesis, Helsinki University of Technology, Department of Forest products technology
3. Hajek B, Esping B (1996) Choosing Green sawing dimensions for various moisture contents after drying. (in Swedish). Institutet för träteknisk forskning, Trätekn
4. Grönlund A, Flodin J, Wamming T (2009) Adaptive control of green target sizes. In: Proceedings of the 19th Wood Machining Seminar, Nanjing Forestry University, Nanjing
5. Ekevad M, Lundgren N, Flodin J (2010) Choosing green sawing dimensions for best value yield of Norway spruce: Industrial measurements and physical modelling. In: Proceedings of the 11th International IUFRO Wood Drying Conference. Luleå University of Technology, Skellefteå, pp 168–173
6. Asmussen S, Glynn PW (2007) Stochastic simulation: algorithms and analysis. Springer, London
7. Danvind J, Ekevad M (2006) Local water vapour diffusion coefficient when drying Norway spruce sapwood. *J Wood Sci* 52:195–201
8. Anonymous (2007) ABAQUS analysis users' manual, version 6.7. Available at <http://www.simulia.com/>. Accessed June 30 2010
9. Ormarsson S (1999) Numerical analysis of moisture-related distortions in sawn timber. Doctoral Thesis, Chalmers University of Technology, Department of Structural Mechanics, Göteborg
10. Ekevad M (2006) Modelling of dynamic and quasistatic events with special focus on wood-drying distortions. Doctoral Thesis, Luleå University of Technology, Division of Wood Science and Technology
11. Anonymous (1999) Wood handbook: Wood as an engineering material. Forest Products Laboratory, US Department of Agriculture, Madison